Effect of crystallographic texture and twinning on the corrosion behavior of Mg alloys: A review

Ehsan Gerashi[1], Reza Alizadeh[1,*], Terence G. Langdon[2]

[1] Department of Materials Science and Engineering, Sharif University of Technology, Tehran, Iran

[2] Materials Research Group, Department of Mechanical Engineering, University of Southampton, Southampton SO17 1BJ, UK

Abstract

Magnesium and its alloys have gained significant popularity due to their light weight and their potential for use as bioresorbable materials. However, their application is limited in practice due to their relatively poor corrosion resistance. Several methods are available for improving the corrosion resistance of Mg alloys for bio-applications such as using different coatings, alloying, and modifying the microstructural parameters such as the grain size and the crystallographic texture. This review provides a comprehensive summary of the effects on the corrosion behavior of crystallographic texture and twinning which represent the main mechanisms of deformation in Mg and Mg alloys. Regarding the crystallographic texture, it is shown that theoretically the basal planes should exhibit a lower corrosion rate but in some cases, such as when there is a galvanic effect or when corrosion films control the overall corrosion behavior, different results may take place. Also, there are contradictory results concerning the effect of twinning on the corrosion behavior. Thus, in some cases twinning may provide preferential sites for corrosion due to the higher energies of atoms located in the twin region by comparison with normal atomic positions in the crystalline lattice whereas there are also other examples where experiments show that twins produce more protective films than in the surrounding matrix.

1. Introduction

In recent years, magnesium alloys have been widely investigated for different applications (as in the automobile industry, metallic implants, electronic devices, etc.) due to their special properties, where the most important are the low density (1.738 g/cm^3), high specific strength, good cast-ability and weld-ability, and reasonable cost. However, poor corrosion resistance of Mg alloys remains an unsolved issue that limits the application of these alloys in applications which need considerable corrosion resistance.

One of the main applications of Mg and Mg alloys which is almost compatible with their poor corrosion resistance, and is of special interest in recent years, is their application as implants in medicine [1]. The regenerative medicine is one of the forefront research fields in healthcare that is now becoming increasingly important as a consequence of the aging and overall longevity of the world's population. In this connection, metallic implants are required for the replacement of tissues having a structural function such as bone and for supporting high stresses where polymeric replacements are not sufficient. With the aim of addressing the disadvantages of permanent metallic implants in the human body, where secondary surgery is often needed to remove the implants from the patient, Mg alloys have gained significant attention in recent years because of their use as biodegradable implants and their potential for providing several favorable properties [2,3].

In practice, there is a long history of using Mg in medical applications because of their biocompatibility and biodegradability [4]. Mg is the lightest structural metal with a density of 1.74 g/cm^3 and an elastic modulus of ~45 GPa, which is only slightly higher than cortical bone. However, pure Mg has a low yield strength of ~30 MPa and a very fast corrosion rate of ~2.89 mm/year [5] with a corrosion potential of about -2.3 V versus standard hydrogen electrode (SHE)

[6] and a hydrogen evolution rate of ~56.5 ml/cm^2/day in simulated body fluid (SBF). By comparison with the desired characteristics for resorbable bone fixtures, such as a compressive strength in the range of 130-180 MPa [7] (similar to compressive strength of the cortical bone, to minimize the stress shielding effect), an elongation higher than ~10 %, a corrosion rate less than ~0.5 mm/year in SBF at 37 °C and a hydrogen evolution of less than 0.48 ml/cm^2/day [8], it appears that pure Mg is too soft and corrodes too quickly within the human body thereby leading to excessive H$_2$ production and a local increase in pH that may cause death of the tissue cells.

It follows therefore that, in order to use Mg in biodegradable applications including reabsorption, it is necessary to develop new Mg alloys with tailored mechanical properties and having appropriate corrosion resistance in physiological environments. Several approaches have been used to overcome these limitations including alloying [9–11] and modifying the microstructure by thermomechanical processing [12]. In practice, thermomechanical processing offers benefits such as a higher strength due to a finer grain size, an enhanced ductility [13], a more uniform distribution of second phase particles [14] and the development of special crystallographic textures [15,16]. These special textures may lead to an increased corrosion resistance by, for example, placing planes having lower surface energy, such as basal planes, at the surface of the deformed samples [17]. In addition, grain refinement can influence the degradability by providing a denser corrosive product layer in the early stages of exposure to the corrosive medium, thereby decreasing the total corrosion rate by further protection of the sub-surface material [18]. While the effects of grain refinement on the corrosion behavior of Mg alloys have been reviewed [19], there are no comprehensive reports or reviews on the effects of the crystallographic texture.

In addition to development of a specific crystallographic texture and also grain refinement, thermomechanical processing, especially at low temperatures, generally results in activation of

2

twinning mode of deformation in Mg and Mg alloys, due to the lack of enough active slip systems in the hcp structure. Twinning, as one of the lattice faults, not only has a great influence on the mechanical properties of metals but also can affect the corrosion behavior [12]. After deformation processing as in rolling and extrusion, twinning is introduced to regulate the texture and microstructure [20,21]. Twinning may also assist slip by the development of new crystallographic orientations as a results of lattice rotation during twinning. For many Mg alloys, the most commonly observed twin modes in Mg alloys are $\{10\bar{1}2\}$ extension twins and $\{10\bar{1}1\}$ contraction twins which are rotated by ~86 °and ~56° from the matrix, respectively [22]. Although the energy of a twin may vary widely depending on its orientation relationship, it is well established that atoms in the twin lattice are more active than those placed on a normal crystallographic plane and this may result in easier corrosion initiation at the twin regions. This seems to be detrimental for the corrosion resistance of Mg alloys, but, as discussed in the following, this is not always the case.

For this reason, the role of crystallographic texture and twinning on the corrosion behavior of Mg alloys needs a much greater clarification and accordingly this limitation is specifically addressed in the present review.

2. Background

2.1. Texture development in Mg alloys

While the crystallographic texture is not usually considered or discussed for as-cast Mg alloys, it is of particular interest and importance for the wrought products. Depending on the mode of plastic deformation, and also the dominant slip system, special textures develop in Mg and Mg alloys after plastic deformation using processes such as rolling [21,23], extrusion [24,25] and also severe plastic deformation (SPD) techniques [26,27]. Regarding extrusion as one of the most

conventional forming techniques for Mg alloys, after extrusion there will be a bar with two directions, the transverse direction (TD) and longitudinal (LD) or extrusion direction (ED) or the extrusion direction (ED). It has been reported that a conventional texture in extruded samples consists of basal planes aligned parallel with the ED. The extrusion parameters such as the speed (or rate) of extrusion, the temperature and also the extrusion ratio can affect the final texture of the extruded bar. In this respect, it was reported that while the Mg-Gd-Y-Zr alloys (GW series) show common extrusion textures at the low extrusion-ratio of 8:1, an unusual extrusion texture is observed in the GW94 alloy at the high extrusion-ratio of 19:1 with the (0001) basal planes aligned perpendicular to the extrusion axis [15]. In addition to deformation parameters, changing composition by the addition of alloying elements such as Ca [28], Al [29], Zn [30], Mn [31], Sr [32] and/or rare earths [33,34] has also been reported to modify the extrusion texture. The alloying elements can weaken or strengthen some specific orientations in the Mg alloys. For example, it was reported that through the addition of Al to an Mg-Mn alloy the basal texture intensity was decreased [35].

2.2. Twinning in Mg alloys

Due to the lack of sufficient active slip systems, twinning is one of the most important deformation mechanisms of Mg and Mg alloys, especially at lower deformation temperatures where there is a very large difference between the critical resolved shear stress (CRSS) for basal slip and for other slip systems such as prismatic and pyramidal. Twinning, as a secondary mode of deformation, contributes less in the total strain by comparison with slip, but instead it enables slip to occur more homogenously by providing new crystallographic orientations as the result of

crystal rotation during twinning. Both mechanical [22] and annealing [36] twins have been observed in Mg alloys.

Atoms are more active on the twin region in comparison with atoms placed on normal lattice sites. Also, different orientation of the lattice in the twinned region in comparison with the surrounding matrix results in some differences in properties which are orientation dependent (like corrosion as discussed in this paper). Noting that usually a considerable volume fraction of twins exists in the microstructure of Mg alloys after plastic deformation, especially at low temperatures, the effect of twinning on the corrosion behavior is clearly important. However, it should be noted that the twin boundaries are not always considered as high energy boundaries. In FCC metals, when the twin boundary is parallel to the twinning plane the atoms in the boundary fit perfectly into both grains and a special boundary called a "coherent twin boundary" is formed, which has extremely low boundary energy. However, this can happen only in the case of the annealing twins and not the mechanical twins, which are the only observed twining mode in Mg alloys.
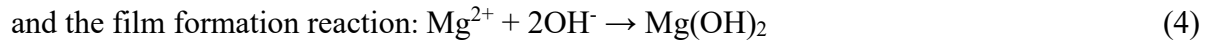

2.3. General corrosion mechanism of Mg alloys

The first reason why Mg has a relatively low corrosion resistance is that it has a high standard electrode potential (about -2.37 V [6]) which makes this element very active and allows it to be susceptible to corrosion even when there is no oxygen. The second reason is that the films (e.g. oxides and hydroxides) formed on the surface of Mg in corrosive medias are usually weak and cannot protect the underlying surface because they are highly defective and soluble in most aqueous solutions [37]. In physiological aqueous environments such as the human body, the corrosion product layers contain MgO (inner thick layer) and $Mg(OH)_2$ (external heavy layer). The former cannot protect the surface as it is not sufficiently dense and the Pilling-Bedworth ratio (the

ratio of molar volume of the elementary unit cell of MgO to that of the Mg metal) is less than 0.8. Also, the latter (Mg(OH)$_2$) is usually dissolved in these environments [7].

Oxygen plays in important role in the atmospheric corrosion, however, in aqueous medias like physiological environments Mg is degraded by an electrochemical reaction with water and in this case Mg(OH)$_2$ and hydrogen gas (H$_2$) is produced. Also, it should be noted that micro-galvanic coupling between the cathodic and anodic areas in aqueous environments is the reason for the corrosion attack. The overall reaction can be described as:

$$Mg+2H_2O \rightarrow Mg(OH)_2 + H_2 \tag{1}$$

However this reaction can be divided into three separate reactions [38] as in

the anodic reaction: $Mg \rightarrow Mg^{2+} + 2\ e^-$ (2)

the cathodic reaction: $2H_2O + 2e^- \rightarrow H_2 + 2OH^-$ (3)

and the film formation reaction: $Mg^{2+} + 2OH^- \rightarrow Mg(OH)_2$ (4)

In the human body, Mg with a high electrochemical potential is more likely to be corroded since a large number of oxygen ions, protein ions and electrolyte ions (such as chloride and hydroxide) are dissolved. This results in the ions migrating from the metal surface to the surrounding body fluid. Normally heavy Mg(OH)$_2$ layers are deposited on the Mg matrix after the occurrence of corrosion (Eq. (3)) [7].

2.4. Surface energy

The "surface free energy" or the "surface energy" or the "interfacial free energy" quantifies the disruption of the interatomic bonds that occurs when a surface is created. The surface energy

may be defined as the excess energy at the surface of a material compared to the bulk or it is the work required to build an area of a particular surface.

Based on the definition of the surface energy given above, in addition to the bonding strength, it will depend also on the numbers of atomic bonds on the proposed surface. In metals with an hcp crystal structure, like Mg, the (0001) basal plane has the highest planar density (1.13 × 10^{19} atoms/m^2) followed by the (11$\bar{2}$0) plane (6.94 × 10^{18} atoms/m^2) and then the (10$\bar{1}$0) plane (5.99 × 10^{18} atoms/m^2) [17]. According to the model based on empirical electron theory, the surface energy of Mg on the (0001), (10$\bar{1}$0) and (11$\bar{2}$0) planes is 1.808, 1.868 and 2.156 eV/nm^2, respectively [39].

Such differences in the surface energy values can obviously affect the corrosion behavior of Mg and Mg alloys in corrosive medias. In theory at least, an atom on a densely packed crystallographic plane has a higher atomic coordination number and thus less available broken bonds when placed on the exterior surfaces of the metal. Therefore, the dissolution of a metallic ion from this plane is expected to be more difficult than from a loosely packed crystallographic plane. In this respect, the basal (0001) planes in Mg should show less tendency to be corroded in different solutions by comparison with the prismatic and pyramidal planes.

2.5. Dissolution rate

The dissolution rate of Mg or its corrosion rate can be correlated to its surface energy. According to detailed reports [40,41], the electrochemical dissolution rate (I_a) may be expressed as:

$$I_a = nFKexp(\frac{Q+\alpha nFE}{RT}) \tag{5}$$

where n is the number of electrons involved in the electrochemical reaction, K is a reaction constant, F is the Faraday constant, R is the universal gas constant, T is the absolute temperature, E is the electrode potential, α is a transfer coefficient if the surface energy, instead of the activation energy, is used in the calculation, and finally Q is an activation energy for a metallic ion to escape from the metal lattice and dissolve into the solution. Thus, Q can simply be associated with the metal (crystal) surface energy Es: $Q = Q_0 - Es$ (where Q_0 is a constant). The surface energy of an exposed crystallographic plane affects Q in the same manner as E and in this regard the activation energy for dissolution of ions from a densely packed surface is higher than a loosely packed surface. Thus, atoms on a lower surface energy plane are dissolved relatively slower.

It can be reasonably assumed that different crystallographic planes have the same n and K values. For example, if different crystallographic planes have the same α, E, n and K, the electrochemical dissolution rates $I_a^{(10\bar{1}0)}$ and $I_a^{(11\bar{2}0)}$ will be in the following form by comparison with the dissolution rate of the basal planes ($I_a^{(0001)}$):

$$I_a^{(10\bar{1}0)} = I_a^{(0001)} \exp\left(\frac{E_s^{(10\bar{1}0)} - E_s^{(0001)}}{RT}\right) \qquad (6)$$

and

$$I_a^{(11\bar{2}0)} = I_a^{(0001)} \exp\left(\frac{E_s^{(11\bar{2}0)} - E_s^{(0001)}}{RT}\right) \qquad (7)$$

It is clear that the dissolution rate of the prismatic $(10\bar{1}0)$ and $(11\bar{2}0)$ planes are much larger than the electrochemical dissolution rate $I_a^{(0001)}$ of the basal plane (0001).

3. Effect of crystallographic texture on the corrosion behavior of Mg alloys

The theoretical dissolution rates of the prismatic $\{10\bar{1}0\}$ and $\{11\bar{2}0\}$ planes are about 18–20 times higher than for the (0001) basal plane [17,40,42–46]. Furthermore, this behavior is not limited to hcp metals and has been reported also for other structures such as fcc metals [47–49]. However, there are also other parameters which may affect the overall behavior. For example, for a surface composed of both prismatic and basal planes, the corrosion resistance is expected to be better than a surface composed only of prismatic planes. Nevertheless, experimental measurements show that this is not correct and the discrepancy has been attributed to galvanic corrosion [50–52] where one metal corrodes preferentially when it is in electrical contact with another metal. This process can occur also in a singular metal (or alloy) in which there is a difference in electrical potential from different constituents within the crystalline matrix such as grains having different orientations. For example, there is a comparison of the transverse and longitudinal surfaces (TS and LS, respectively) of an as-extruded Mg–3Al–1Zn (AZ31) alloy where the electron back scattered diffraction (EBSD) data are shown in Fig.1 [50,51]. According to these results, corrosion may occur easily in the $\{10\bar{1}0\}$ and $\{11\bar{2}0\}$ oriented grains when galvanized with the (0002) oriented grains and this means that having both of them simultaneously may enhance the corrosion resistance due to the galvanic effect between the basal and prismatic planes. Hence, when the surface is composed entirely of (0002) basal planes or $\{10\bar{1}0\}$ and $\{11\bar{2}0\}$ prismatic planes the galvanic corrosion due to grain misorientation may be avoided at least to a large extent.

In another study on the same AZ31 alloy [51] it was shown that not only the corrosion behavior of the base material was dependent upon the crystallographic texture but also the protectiveness of the corrosive film depended on the orientation of the planes. For the surface containing a highly concentrated orientation of $\{10\bar{1}0\}$ and $\{11\bar{2}0\}$ prismatic planes, it was observed that the degradation of the formed corrosive film was relatively minor and only occurred

at some particular sites after an immersion for 48 h in a phosphate buffer saline (PBS) medium. This means that the film maintained a good corrosive protection for the underlying substrate. However, for the surface containing {0002} basal planes together with {10$\bar{1}$0} and {11$\bar{2}$0} prismatic planes, the degradation of the corrosive product film occurred more widely and this led to a further decrease in the corrosion resistance of the immersed samples. The effect of crystallographic texture on the formation of passive films is discussed in more details in section 3.1.

As was discussed earlier, the most important impact of the crystallographic orientation is on the anodic dissolution of metals. However, it has been shown that different crystallographic planes with different energies can also influence the cathodic hydrogen evolution process (Eq. 3 in section 2.3). This means that a surface with a higher energy leads to more adsorption of water or protons and thus a hydrogen evolution reaction. However, the influence of the surface energy is indirect and hence less significant on the activation energy of the hydrogen reaction than that for metal dissolution [40,53]. In fact, the orientation dependence of the current density is almost negligible in the cathodic region (in the polarization curve) [44].

Another interesting finding from the polarization curve measurements is that the open circuit potential (OCP) of the closely packed (0001) surface is more positive than that of the less densely packed (10$\bar{1}$0) and (11$\bar{2}$0) surfaces. An implication of the different OCPs is that micro-galvanic cells will be formed between grains with different orientations. Such a micro-galvanic effect can lead to preferential dissolution of the (10$\bar{1}$0) and (11$\bar{2}$0) orientated grains [40].

As already noted, the crystallographic texture can significantly influence the corrosion behavior of Mg alloys. However, in many cases it is difficult to completely isolate the effect of texture from other metallurgical parameters such as the effect of intermetallic phases, grain size,

film formation on the surface and the dislocation density. For example, it was reported that the electrochemical galvanic effect of the intermetallic particles suppresses the influence of the crystallographic orientation and leads to a diminished difference in corrosion behavior between the rolling surface and cross-sectional surfaces [41]. In the following, cases are discussed where the main focus is on the effect of crystallographic texture or twining on the corrosion resistance.

3.1. Film formation

In general, the overall corrosion behavior of a metal depends on the corrosion behavior of both the substrate and the film. It has been shown that different oxide films can markedly alter the corrosion behavior of Mg alloys [37,54–59]. The process of film formation on a metal surface depends not only on the environment facing the metal but also on the metallurgical properties of the substrate including the grain size and the crystallographic texture, where the latter example is of particular interest in the present paper.

Regarding the effect of crystallographic texture on the corrosion film and thus on the overall corrosion behavior of Mg alloys, two possible facts should be considered: (1) the surface films on different grains are almost the same in composition and microstructure, but they are not compact or resistant enough to effectively conceal the difference of the substrate grain orientation in corrosion; (2) the surface film varies from grain to grain in compactness and resistance due to the different film formation processes on the grains with different electrochemical activities. This means that, while the corrosivity of a solution decreases or the passivity of the metal increases, the surface films on different grains tend to become thinner, more compact, more resistant and more uniform (and so less different), and their ability to conceal the grain orientation influence improves.

In a corrosive solution, both substrate grain orientation and surface film affect the overall Mg corrosion behavior. In such cases, the substrate grain orientations are considered as primarily responsible for the different corrosion performances and the different surface films on the grains which can further enlarge these differences. In a strong passivating or less aggressive solution, although the difference between films on different grains becomes small, their high corrosion resistance can significantly reduce the activity of the substrate grains and therefore reduce or even eliminate the grain orientation effect on the corrosion performance. If a solution contains a stronger passivator, such as chromate, to form a very thin and compact film, but also includes aggressive species like chloride ions to enlarge any localized difference in the film and substrate grains, then a different corrosion behavior will be expected. The Cl$^-$ ions will selectively attack the film formed along dislocations, twins and grain boundaries because they have atomic arrangements or crystal orientations that are very different from the bulk grain. Furthermore, chromates stabilize the surface film to prevent overall or uniform corrosion development. In such a solution, the competition between corrosive and passivating species in defects and bulk grains will lead to different corrosion morphologies and filiform damage [60] which will be discussed in another section.

It was reported that the basal plane in pure Mg develops a slightly thinner but perhaps slightly more compact film by comparison with the prismatic plane in both an Mg(OH)$_2$ saturated solution and a 1 M NaOH solution [60]. The formation of thinner oxide films on basal planes was also reported for other hcp metals such as Ti and Zr. In the case of Zr, the oxidation rate of the basal plane was slower than that of the prismatic planes, and this difference was attributed to the different oxygen diffusion kinetics through the high packed and low packed planes [61,62]. In another study on pure Mg [63], a notable dependency of the thickness of the oxide film on the

crystallographic texture was reported in different solutions. In all studied environments, the thinnest and thickest oxide films were formed on the basal planes and the low index planes, respectively, while the thickness of this oxide was inversely proportional to the corrosion rate.

In addition to film thickness, the nature of the film may be different also on grains with different crystallographic orientations. Thus, it was reported that the Pilling-Bedworth (PB) ratio, which is used to describe the effectiveness of an oxide film, varies with crystallographic orientation and increases with atomic density in pure Mg. The value of PB for the sample with the higher amount of basal plane or (0002) oriented grains is higher than for other samples. This suggests that the stability of the corrosion film and the corrosion resistance in the basal planes would be improved [45]. Also, an incorporation of an MgO and $Mg(OH)_2$ passive film (in a 3.5 wt.% NaCl solution) on pure Mg surfaces with low-index planes is facilitated and could enhance the corrosion resistance by forming a more effective barrier against the penetration of chloride ions [64].

Finally, it can be concluded that in the surfaces containing basal planes the formed oxide film is always thinner by comparison with that formed on the pyramidal or prismatic planes but there is a contrary result about their stability and effectiveness. In Table 1, the effect of texture on the film formation is summarized for the corrosion of Mg and its alloys in corrosive media. In this summation, the effect of texture on the corrosion film (given in the fourth column from the left) is summarized for different materials (first column) in different solutions (second column) and then evaluated by different methods (third column) from the available references (last column).

3.2. Filiform corrosion

Filiform corrosion often occurs on the surface of metals such as steel, aluminum alloys and Mg alloys and it is caused by active galvanic cells across the metal surface [65]. The filiform

corrosion of Mg alloys is a common type of corrosion [66–69] and occurs on bare Mg alloy surfaces exposed to air and NaCl solution [70]. For example, Fig 2. shows the orientation dependent morphologies of corrosion in pure Mg exposed to 0.6 M NaCl (after the samples were cleaned with CrO_3). The filiform corrosion was observed on the low index plane $\{01\bar{1}0\}$ whereas other higher index grains displayed terraces instead of this filiform type morphology [63]. However, in solutions containing both chloride and dichromate, pure Mg is susceptible to localized corrosion in the form of filaments that can propagate at very high rates [71]. In Mg alloys, the pitting and filiform type corrosion usually occur at the same time. The filiform corrosion initiates from pits and extends along the active areas. In corrosion of Mg alloys, the hydrogen plays a more vital role in comparison with the oxygen (unlike many other alloys such as steels), as was described in section 2.3. The filiform corrosion of Mg is due to the difference in oxygen concentration between the filament head and the filament tail, and this suggests a filiform corrosion model for the Mg alloys [70]. It has been reported that the filiform corrosion in Mg alloys is strongly orientation dependent [71,72].

The presence of dichromate ions in the solution effectively increases the corrosion resistance of the Mg surface. However, in a solution containing both chloride and dichromate, Mg is susceptible to localized corrosion in the form of filaments that can propagate at very high rates where these filaments are called filiform corrosion and are shown in Fig. 3 [71]. The corrosion behavior of Mg in 0.01 M Cl^- solutions containing small additions of dichromate (10^{-4} M) results in a localized filiform attack. Based on the experimental results, this localized pitting has been shown to be dependent on the crystallographic texture where the Mg (0001) basal plane surface exhibits the least resistance to localized attack [72]. In practice, the Mg (0001) surface exhibits corrosion susceptibility at its open circuit corrosion potential. However, the prismatic surfaces of $(10\bar{1}0)$

and $(11\bar{2}0)$ are passive under open circuit conditions and localized attack is initiated only upon polarization to potentials slightly anodic to their open circuit potentials. The critical pitting potential for Mg single crystals increases in the order of $(0001) < (10\bar{1}0) < (11\bar{2}0)$. The localized attack on all three surfaces is associated with the formation and propagation of corrosion filaments exhibiting a crystallographic directional dependence [72]. It should be noted here that these results are showing the crystallographic dependency for the pitting susceptibilities of Mg single crystals in a special environment $(0.01\ M\ NaCl + 10^{-4}\ M\ Na_2Cr_2O_7)$ considered specifically for increasing pitting. This is different from the general corrosion behavior described in section 3, in normal Cl^- containing solutions (without the dichormomat ions). The observed differences between the pitting susceptibility of the basal plane and prismatic planes in Mg single crystals [72] is reported to agree well with the findings reported for corrosion of polycrystalline Mg in the same solution. Findings were reported [71] from immersion experiments for polycrystalline Mg, indicating that pitting was only observed on grains closely oriented near the {0001} family of surfaces as verified by optical imaging microscopy. In that work, the attacked grains exhibited corrosion that propagated as filaments similar to those observed on the Mg (0001) surfaces.

3.3. Biocompatibility

While there are some reports on the dependency of biocompatibility on crystallographic texture in hcp metals [73–75], this effect is not well examined and the outcome is not clear in the case of Mg and Mg alloys. For example, it was reported that the number of attached cells was higher on the surface of titanium samples having more (0002) planes parallel to the surface regardless of the sample grain size. It was found that a higher density of cells attached on the samples with stronger basal texture and this was related to the modified nature of the oxide film

formed on those surfaces [73,74]. Also, in an investigation of the effect of crystallographic texture of the other similar HCP alloys like Ti-6Al-4V on cell attachment, it was reported that there was an improved cell attachment and proliferation onto the substrate with a predominantly $(10\bar{1}0)$ exposed surface by comparison with $(11\bar{2}0)$ [75]. This behavior was attributed to the lower surface contact angle of the $(10\bar{1}0)$ orientation and accordingly to the higher wettability, as it was shown that increased surface wettability or hydrophilicity may enhance protein adsorption and cell spreading on biomaterials [76–78]. By contrast, there are some reports indicating that the biocompatibility of pure Mg is less sensitive to texture [46]. In this respect, there are some investigations which have studied the effect of different thermo-mechanical processing on the biocompatibility. Although these reports are not considered directly, the obtained results show indirectly that biocompatibility of the Mg alloys is not significantly affected by the texture since it is reasonable to assume that different textures are obtained after different thermos-mechanical routes [79–81]. Accordingly, it can be concluded that the mechanical properties and resorption rates of Mg alloys may be tuned through control of the texture without too much loss of biocompatibility. However, it is readily apparent that further research is required in this area.

4. Effect of twinning on the corrosion behavior of Mg alloys

Although the energy of a twin may vary widely depending on its orientation relationship, it is readily apparent that atoms in a twin lattice are more active than in a normal crystallographic plane [41]. Therefore, it is expected that the existence of twins on exterior surfaces will have negative effects on the corrosion behavior. In practice, there are several studies which support this hypothesis and show an increased corrosion rate of the base Mg alloy in the presence of twins. For example, applying the equal channel angular extrusion (ECAE) process on an AZ31 alloy showed

that, while the grain size hardly changed, a higher density of dislocations and twins appeared which led to a sharp increase in the corrosion rate [82]. In another study investigating the corrosion behavior of a rolled AZ31B alloy, heat treatment at different temperatures was used to obtain different microstructures with and without twins [83]. According to the results of this study, the corrosion was more serious for the highly twinned microstructures of the as-received samples and samples heat treated at 200°C compared with coarse-grained samples heat treated at 300°C which contained almost no twins. Figure 4 shows the optical micrographs of these two samples [83]. Also, the closed-up corroded surface of the as-received microstructure suggests that twins further accelerated the intragranular corrosion. Based on these experiments, a higher density of dislocations and twins probably leads to high hardness values and high anodic dissolution. The acceleration of anodic metal dissolution is caused by a local reduction of the equilibrium potential in the vicinity of dislocations. However, the main drawback of this work is that the effect of grain size was not considered.

Interestingly, there are also some reports indicating that twinning can increase the corrosion resistance. These contrary reports may occur because in different alloying systems the corrosion films have different abilities to protect the underlying matrix. For example, the effect of extension twinning on the corrosion properties of an Mg-1Y alloy was studied by eliminating the effects of secondary particles, maintaining the same grain size and also weakening the effect of crystal orientation [84]. It was found that the presence of extension twinning greatly influences the corrosion process by increasing the pitting potential, film formation and the charge transfer resistance, leading to an improvement in the overall electrochemical corrosion properties. The surface energy of atoms on the $\{10\bar{1}2\}$ extension twinning plane was found to be higher than in the $\{0001\}$ closely-packed basal plane due to a lower coordination number. This indicates that the

atoms in the extension twinning planes possess higher oxidization activity and this gives a preferential formation of oxidation film. This oxide film can effectively prevent the solution medium from touching the surface of the Mg-1Y alloy which leads to a larger charge transfer resistance as was further confirmed later [85]. Accordingly, the oxide film can be preferentially formed on the twinning plane with a higher oxidation activity and thus an increase in the charge transfer resistance.

For the Mg–4Zn alloy [12], it was confirmed that on the twinning planes the stress concentrations at the grain-twin interfaces have adverse effects on the corrosion resistance, but a compact oxide layer may be formed on the twinning plane which improves the overall corrosion resistance. It can be inferred from Fig. 5 that the grains containing twins, marked by arrows, have become slightly corroded by comparison with other similarly oriented grains without twins. Thus, it appears that an optimum volume fraction of twins is preferred in order to improve the corrosion behavior of the Mg–4Zn alloy [12].

Another contribution of twinning in the corrosion process can be its weakening effect on the "corrosion anisotropy". Applying thermo-mechanical processing, as in extrusion and rolling, normally causes corrosion anisotropy in Mg and its alloys, meaning that different directions (like TD, ND, RD after rolling) will exhibit different corrosion behaviors. After the rolling process, pre-straining the surfaces of the rolled plate by compression can introduce a large amount of twinning in the structure and thus influence the corrosion anisotropy between differently oriented surfaces [86]. Twin boundaries are fully coherent and have lower interfacial energies than those of the incoherent grain boundaries. For example, for pure magnesium the energy of the $\{10\bar{1}2\}$ extension twin boundary is 0.11–0.20 J/m^2 which is far lower than the grain boundary energy (0.41–0.60 J/m^2). Moreover, due to the activation of high densities of $\{10\bar{1}2\}$ twins in the pre-strained

samples, the formed twin boundaries and original grain boundaries may remarkably increase the quantity of physical barriers to any corrosion attack. After being pre-strained, the growth and development of localized corrosion are effectively delayed or retarded. In addition, high densities of $\{10\bar{1}2\}$ twins may be simultaneously activated in differently oriented samples after a 3% compressive stain along the rolling direction of the plate. Thus, the beneficial effect of twin boundaries on any weakening corrosion attack is the same for differently oriented surfaces. Following this, the corrosion anisotropy in as-rolled AZ31 Mg alloys with strong basal textures can be remarkably weakened due to the high densities of activated twins. Based on the description mentioned above, this demonstrates that the formation of high densities of $\{10\bar{1}2\}$ twins could be an effective way for simultaneously weakening the corrosion anisotropy and thereby improving the corrosion resistance of wrought Mg alloys.

In addition to experimental studies, the effect of twin boundaries (TB) on the anodic dissolution of Mg was also investigated theoretically [87] and it was found that twin boundaries (TB1 $\{10\bar{1}1\}$ $[1\bar{2}10]$, TB2 $\{10\bar{1}2\}$ $[1\bar{2}10]$, or TB3 $\{10\bar{1}3\}[1\bar{2}10]$) accelerate the corrosion rate such that the accelerations of the current density is related to the TB interfacial length per area. This behavior was attributed to the fact that TBs in the microstructure increase the surface energy density.

Contrary to some reports on the great influence of twinning on the corrosion behavior, there are also some studies suggesting that twinning generally has no great influence on the corrosion behavior of Mg alloys. For example, in an investigation of a rolled and heat treated AZ31 alloy it was reported that twinning played no decisive role in the corrosion behavior [41]. The effect of twining is therefore discussed in more detail in the following sections.

4.1. Direct role (galvanic effect)

The corrosion behavior of two samples having different orientations (transverse cross-section, TS, and longitudinal cross-section, LS) was compared in an as-extruded Mg–3Al–1Zn bar [50]. It was shown that the corrosion attack in an orientation with a high fraction of twins (TS) was weaker than in an orientation with a low fraction of twins (LS). This means that the activation of $\{10\bar{1}2\}$ twinning can cause localized galvanic corrosion in some twinned areas but cannot induce a significant effect on the corrosion performance of the TS sample. This research firmly demonstrates that whenever the exterior surface is mainly composed of prismatic planes then the galvanic corrosion occurring between the twinned and untwinned areas can be weakened.

In another study [88], an Mg-5Y-7Gd-1Nd-0.5Zr (EW75 alloy) was compressed to obtain twins under a T3 treatment (compressed at room temperature) and this condition was compared with the solid solution treated samples with no twins (T4). Optical microscopy images of T3 and T4 samples are shown in Fig. 6. It was found that in a corrosive solution the twins play a dual role. Accordingly, the micro-galvanic corrosion between twins accelerates the corrosion rate and simultaneously promotes the formation of a surface film. However, the formation of a compact surface film was more effective in an EW75 alloy. As a result, the twins in the EW75 alloy can improve the corrosion resistance. This dual effect was also further confirmed in another study [89] where the effect of twins on the corrosion behavior was investigated for ZK60. The results showed that a small volume fraction of twins could decrease the corrosion resistance due to a galvanic effect while a high density of twins could improve the corrosion resistance of the material due to the preferential formation of an oxidation film (MgO).

In Table 2, the effect of twinning on the corrosion behavior is summarized. Thus, the effect of twinning on the corrosion resistance (fifth column from the left) is summarized for different materials (first column) prepared by different processes (second column), in different solutions

20

(third column), and evaluated by different methods (fourth column) from the available references (last column).

4.2. The role of twinning shape in corrosion propagation in solutions containing dichromate

A study was initiated to examine the corrosion behavior of pure Mg in a dichromate containing solution [71]. On a large-grained sample, the attack was observed to propagate at the twin boundaries. Orientation imaging microscopy analysis found that corrosion was limited to planes near {0001} orientations with propagation lying in the prismatic directions. After polishing the large-grain sample, defects such as twins, subtwins, and grain boundaries, were visible in the microscopic images. The interaction of twins and the corrosion path can be observed in Fig. 7 [71]. A filiform-like corrosion, about 1 mm wide, developed at a twin in Fig. 7a and followed the twin until it intersected another twin. The corrosion filament crossed the other twin and then followed it in Fig. 7b. It is interesting to note that the propagation of the corrosion was strongly influenced by the presence of the twins but it was not influenced by the subtwins. This result suggests that the filiform type corrosion may also follow the defects such as twins of smaller size within the grains of the small grain sample.

In Fig. 8 it is shown that the corrosion filaments interact with twins [71]. When the twins are thin by comparison to the width of the filament, there is little or no influence on the propagation direction and propagation continues in the grain in the same direction. However, when the twins are thick, the corrosion filament changes direction and continues to grow in the grain but not through the twin.

5. Summary and overall outlook

Magnesium is an active metal and the corrosion rate of Mg and Mg alloys is normally too high for most applications. There are some ways to control and decrease the corrosion rate, such as applying coatings, changing the chemical composition through the addition of alloying elements and/or by modifying the microstructure as in decreasing the grain size, introducing twins or changing the crystallographic texture. Among the possible controllable microstructural parameters, the effect of crystallographic texture and twinning on the corrosion behavior of pure Mg and its alloys has been reviewed in this paper. The most important conclusions may be effectively summarized as follows:

1. Theoretically, the basal planes have the most corrosion resistance among all the crystallographic planes. However, there are also contrary results mainly originating from the galvanic effect or the formation of more stable films on the non-basal planes which reduce the overall corrosion rate.

2. In addition to the corrosion behavior of the base material, the film formation process is also orientation dependent. The thickness and also the nature of the films depend on the crystallographic texture. In most cases, thinner but more compact films are formed on the basal planes by comparison with the less compact prismatic and pyramidal planes.

3. The effect of twinning on the corrosion behavior is complex and several results are contradictory. There are results confirming the deleterious effect of twins on the corrosion behavior but there are also other reports indicating an improved corrosion resistance in the presence of twins due the formation of a better protective layer. In addition to this duality, there are data reporting galvanic corrosion between the twinned and untwined areas. The overall effect seems to be strongly composition dependent. In alloys with a stable protective film, like Mg-Y

alloys, the presence of twinning can increase the corrosion resistance. Twining was also reported to reduce the corrosion anisotropy in wrought samples.

4. The filiform-type corrosion is orientation dependent and is influenced also by the presence of twins in the microstructure. The available results suggest that the corrosion filaments interact differently with thin twins, thick twins and with sub-twins.

References:

[1]   Y. Yang, X. Xiong, J. Chen, X. Peng, D. Chen, F. Pan, Research advances in magnesium and magnesium alloys worldwide in 2020, J. Magnes. Alloy. 9 (2021) 705–747.

[2]   F. Kiani, C. Wen, Y. Li, Prospects and strategies for magnesium alloys as biodegradable implants from crystalline to bulk metallic glasses and composites—A review, Acta Biomater. 103 (2020) 1–23.

[3]   N. Sezer, Z. Evis, S.M. Murat, A. Tahmasebifar, M. Koç, Review of magnesium-based biomaterials and their applications, J. Magnes. Alloy. 6 (2018) 23–43.

[4]   F. Witte, The history of biodegradable magnesium implants: A review, Acta Biomater. 6 (2010) 1680–1692.

[5]   H. R. Bakhsheshi-Rad, M.H. Idris, M.R. Abdul-Kadir, A. Ourdjini, M. Medraj, E. Hamzah, Mechanical and bio-corrosion properties of quaternary Mg-Ca-Mn-Zn alloys compared with binary Mg-Ca alloys, Mater. Des. 53 (2014) 283–292.

[6]   J. Xie, J. Zhang, Z. You, S. Liu, K. Guan, R. Wu, J. Wang, J. Feng, Towards developing Mg alloys with simultaneously improved strength and corrosion resistance via RE alloying, J. Magnes. Alloy. 9 (2021) 41–56.

[7]   Y. Yang, C. He, E. Dianyu, W. Yang, F. Qi, D. Xie, L. Shen, S. Peng, C. Shuai, Mg bone implant : Features , developments and perspectives, Mater. Des. 185 (2020) 108259.

[8]   M. Erinc, W.H. Sillekens, R.G.T.M. Mannens, R.J. Werkhoven, Applicability of existing magnesium alloys as biomedical implant materials, In: E.A. Nyberg, S.R. Agnew, N.R. Neelameggham, M.O Pekguleryuz (eds) Magnesium. Technology, TMS (The Minerals and Materials Society), Pa, USA (2009) 209–214.

[9]   M. Sabbaghian, R. Mahmudi, K.S. Shin, Microstructure , texture , mechanical properties and biodegradability of extruded Mg – 4Zn – x Mn alloys, Mater. Sci. Eng. A. 792 (2020) 139828.

[10]   C. Li, Y. He, H. Huang, Effect of lithium content on the mechanical and corrosion behaviors of HCP binary Mg–Li alloys, J. Magnes. Alloy. 9 (2021) 569–580.

[11]   A. Gungor, A. Incesu, Effects of alloying elements and thermomechanical process on the mechanical and corrosion properties of biodegradable Mg alloys, J. Magnes. Alloy. 9 (2021) 241–

253.

[12]   M. Sabbaghian, R. Mahmudi, K.S. Shin, Effect of texture and twinning on mechanical properties and corrosion behavior of an extruded biodegradable Mg–4Zn alloy, J. Magnes. Alloy. 7 (2019) 707–716.

[13]   R. Alizadeh, R. Mahmudi, A.H.W. Ngan, Y. Huang, T.G. Langdon, Superplasticity of a nano-grained Mg-Gd-Y-Zr alloy processed by high-pressure torsion, Mater. Sci. Eng. A. 651 (2016) 786–794.

[14]   R. Alizadeh, R. Mahmudi, A.H.W. Ngan, T.G. Langdon, Microstructural evolution during hot shear deformation of an extruded fine-grained Mg-Gd-Y-Zr alloy, J. Mater. Sci. 52 (2017) 7843–7857.

[15]   R. Alizadeh, R. Mahmudi, A.H.W. Ngan, T.G. Langdon, An Unusual Extrusion Texture in Mg-Gd-Y-Zr Alloys, Adv. Eng. Mater. 18 (2016) 1044–1049.

[16]   D. Ahmadkhaniha, Y. Huang, M. Jaskari, A. Järvenpää, M.H. Sohi, C. Zanella, L.P. Karjalainen, T.G. Langdon, Effect of high-pressure torsion on microstructure, mechanical properties and corrosion resistance of cast pure Mg, J. Mater. Sci. 53 (2018) 16585–16597.

[17]   M. Liu, D. Qiu, M.C. Zhao, G. Song, A. Atrens, The effect of crystallographic orientation on the active corrosion of pure magnesium, Scr. Mater. 58 (2008) 421–424.

[18]   Y. Xin, C. Liu, X. Zhang, G. Tang, X. Tian, P.K. Chu, Corrosion behavior of biomedical AZ91 magnesium alloy in simulated body fluids, J. Mater. Res. 22 (2007) 2004–2011.

[19]   K.D. Ralston, N. Birbilis, Effect of grain size on corrosion: A review, Corrosion. 66 (2010) 0750051–07500513.

[20]   Y.J. Kim, J.U. Lee, Y.M. Kim, S.H. Park, Microstructural evolution and grain growth mechanism of pre-twinned magnesium alloy during annealing, J. Magnes. Alloy. (2020).

[21]   L.L.C. Catorceno, H.F.G.D. Abreu, A. F. Padilha, Effects of cold and warm cross-rolling on microstructure and texture evolution of AZ31B magnesium alloy sheet, J. Magnes. Alloy. 6 (2018) 121–133.

[22]   T. Liu, Q. Yang, N. Guo, Y. Lu, B. Song, Stability of twins in Mg alloys – A short review, J. Magnes. Alloy. 8 (2020) 66–77.

[23]   Q. Li, G.J. Huang, X.D. Huang, S.W. Pan, C.L. Tan, Q. Liu, On the texture evolution of Mg–Zn–Ca

alloy with different hot rolling paths, J. Magnes. Alloy. 5 (2017) 166–172.

[24]   Y.P Wang, F. Li, Y. Wang, X. w Li, W. W. Fang, Effect of extrusion ratio on the microstructure and texture evolution of AZ31 magnesium alloy by the staggered extrusion (SE), J. Magnes. Alloy. 8 (2020) 1304–1313.

[25]   X. Che, Q. Wang, B. Dong, M. Meng, Z. Gao, K. Liu, J. Ma, F. Yang, Z. Zhang, The evolution of microstructure and texture of AZ80 Mg alloy cup-shaped pieces processed by rotating backward extrusion, J. Magnes. Alloy. (2021).

[26]   X. Zhao, S. Li, Z. Zhang, P. Gao, S. Kan, F. Yan, Comparisons of microstructure homogeneity, texture and mechanical properties of AZ80 magnesium alloy fabricated by annular channel angular extrusion and backward extrusion, J. Magnes. Alloy. 8 (2020) 624–639.

[27]   W. Yang, G.F. Quan, B. Ji, Y.F. Wan, H. Zhou, J. Zheng, D.D. Yin, Effect of Y content and equal channel angular pressing on the microstructure, texture and mechanical property of extruded Mg-Y alloys, J. Magnes. Alloy. (2020).

[28]   H.L. Ding, P. Zhang, G.P. Cheng, S. Kamado, Effect of calcium addition on microstructure and texture modification of Mg rolled sheets, Trans. Nonferrous Met. Soc. China (English Ed). 25 (2015) 2875–2883.

[29]   X. Zheng, W. Du, K. Liu, Z. Wang, S. Li, Effect of trace addition of al on microstructure, texture and tensile ductility of Mg-6Zn-0.5Er alloy, J. Magnes. Alloy. 4 (2016) 135–139.

[30]   D.W. Kim, B.C. Suh, M.S. Shim, J.H. Bae, D.H. Kim, N.J. Kim, Texture evolution in Mg-Zn-Ca alloy sheets, Metall. Mater. Trans. A Phys. Metall. Mater. Sci. 44 (2013) 2950–2961.

[31]   L. Chunquan, C. Xianhua, C. Jiao, A. Atrens, P. Fusheng, The effects of Ca and Mn on the microstructure, texture and mechanical properties of Mg-4 Zn alloy, J. Magnes. Alloy. 9 (2020) 1084-1097.

[32]   M. Masoumi, M. Pekguleryuz, The influence of Sr on the microstructure and texture evolution of rolled Mg-1%Zn alloy, Mater. Sci. Eng. A. 529 (2011) 207–214.

[33]   D. Guan, X. Liu, J. Gao, L. Ma, B.P. Wynne, W.M. Rainforth, Exploring the mechanism of "Rare Earth" texture evolution in a lean Mg–Zn–Ca alloy, Sci. Rep. 9 (2019) 1–11.

[34]   A. Imandoust, C.D. Barrett, T. Al-Samman, K.A. Inal, H. El Kadiri, A review on the effect of rare-

earth elements on texture evolution during processing of magnesium alloys, J. Mater. Sci. 52 (2017) 1-29.

[35]   M.Z. Bian, A. Tripathi, H. Yu, N.D. Nam, L.M. Yan, Effect of aluminum content on the texture and mechanical behavior of Mg-1wt% Mn wrought magnesium alloys, Mater. Sci. Eng. A. 639 (2015) 320–326.

[36]   L.Y. Sheng, B.N. Du, Z.Y. Hu, Y.X. Qiao, Z.P. Xiao, B.J. Wang, D.K. Xu, Y.F. Zheng, T.F. Xi, Effects of annealing treatment on microstructure and tensile behavior of the Mg-Zn-Y-Nd alloy, J. Magnes. Alloy. 8 (2020) 601–613.

[37]   M. Esmaily, J.E. Svensson, S. Fajardo, N. Birbilis, G.S. Frankel, S. Virtanen, R. Arrabal, S. Thomas, L.G. Johansson, Fundamentals and advances in magnesium alloy corrosion, Prog. Mater. Sci. 89 (2017) 92–193.

[38]   G.L. Song, A. Atrens, Corrosion Mechanisms of Magnesium Alloys, Adv. Eng. Mater. 1 (2000) 11–33.

[39]   B.Q. Fu, W. Liu, Z.L. Li, Calculation of the surface energy of hcp-metals with the empirical electron theory, Appl. Surf. Sci. 255 (2009) 9348–9357.

[40]   G.L. Song, R. Mishra, Z. Xu, Crystallographic orientation and electrochemical activity of AZ31 Mg alloy, Electrochem. Commun. 12 (2010) 1009–1012.

[41]   G.L. Song, Z. Xu, Effect of microstructure evolution on corrosion of different crystal surfaces of AZ31 Mg alloy in a chloride containing solution, Corros. Sci. 54 (2012) 97–105.

[42]   R. Xin, B. Li, L. Li, Q. Liu, Influence of texture on corrosion rate of AZ31 Mg alloy in 3.5wt.% NaCl, Mater. Des. 32 (2011) 4548–4552.

[43]   H. Torbati-Sarraf, S.A. Torbati-Sarraf, A. Poursaee, T.G. Langdon, Electrochemical behavior of a magnesium ZK60 alloy processed by high-pressure torsion, Corros. Sci. 154 (2019) 90–100.

[44]   G.L. Song, The effect of texture on the corrosion behavior of AZ31 Mg alloy, Jom. 64 (2012) 671–679.

[45]   K. Hagihara, M. Okubo, M. Yamasaki, T. Nakano, Crystal-orientation-dependent corrosion behaviour of single crystals of a pure Mg and Mg-Al and Mg-Cu solid solutions, Corros. Sci. 109 (2016) 68–85.

[46]   S. Bahl, S. Suwas, K. Chatterjee, The control of crystallographic texture in the use of magnesium as a resorbable biomaterial, RSC Adv. 4 (2014) 55677–55684.

[47]   B.R. Kumar, R. Singh, B. Mahato, P.K. De, N.R. Bandyopadhyay, D.K. Bhattacharya, Effect of texture on corrosion behavior of AISI 304L stainless steel, Mater. Charact. 54 (2005) 141–147.

[48]   S.S. Chouthai, K. Elayaperumal, Texture dependence of corrosion of mild steel after cold rolling, Br. Corros. J. 11 (1976) 40–43.

[49]   D.J. Horton, A.W. Zhu, J.R. Scully, M. Neurock, Crystallographic controlled dissolution and surface faceting in disordered face-centered cubic FePd, MRS Commun. 4 (2014) 113–119.

[50]   B.J. Wang, D.K. Xu, J.H. Dong, W. Ke, Effect of the crystallographic orientation and twinning on the corrosion resistance of an as-extruded Mg-3Al-1Zn (wt.%) bar, Scr. Mater. 88 (2014) 5–8.

[51]   B. Wang, D. Xu, J. Dong, W. Ke, Effect of Texture on Biodegradable Behavior of an As-Extruded Mg–3%Al–1%Zn Alloy in Phosphate Buffer Saline Medium, J. Mater. Sci. Technol. 32 (2016) 646–652.

[52]   J. Peng, Z. Zhang, C. Long, H. Chen, Y. Wu, Effect of crystal orientation and f 1012 g twins on the corrosion behaviour of AZ31 magnesium alloy, J. Alloys Compd. 827 (2020) 154096.

[53]   Q. Jiang, X. Ma, K. Zhang, Y. Li, X. Li, Y. Li, M. Ma, B. Hou, Anisotropy of the crystallographic orientation and corrosion performance of high-strength AZ80 Mg alloy, J. Magnes. Alloy. 3 (2015) 309–314.

[54]   N. Hara, Y. Kobayashi, D. Kagaya, N. Akao, Formation and breakdown of surface films on magnesium and its alloys in aqueous solutions, Corros. Sci. 49 (2007) 166–175.

[55]   S. Leleu, B. Rives, J. Bour, N. Causse, N. Pébère, On the stability of the oxides film formed on a magnesium alloy containing rare-earth elements, Electrochim. Acta. 290 (2018) 586–594.

[56]   Y. Song, E.H. Han, K. Dong, D. Shan, C.D. Yim, B.S. You, Microstructure and protection characteristics of the naturally formed oxide films on Mg-xZn alloys, Corros. Sci. 72 (2013) 133–143.

[57]   R.B. Figueiredo, T.G. Langdon, Processing Magnesium and Its Alloys by High-Pressure Torsion : An Overview, 1801039 (2019) 1–15.

[58] G.L. Song, P.E. Gannon, The surface films and their possible roles in Mg corrosion. In: A. Singh, K. Solanki, M.V. Manuel, N.R Neelameggham (Eds) Magnesium Tehchnology (2016) Springer, Cham.

[59] J.H. Nordlien, S. One, N. Masuko, Morphology and Structure of Oxide Films Formed on Magnesium by Exposure to Air and Water, 142 (1995) 3320–3322.

[60] G.L. Song, Z. Xu, Crystal orientation and electrochemical corrosion of polycrystalline Mg, Corros. Sci. 63 (2012) 100–112.

[61] U. Konig, B. Davepon, Microstructure of polycrystalline Ti and its microelectrochemical properties by means of electron-backscattering diffraction (EBSD), Electrochim. Acta. 47 (2001) 149–160.

[62] H.G. Kim, T.H. Kim, Y.H. Jeong, Oxidation characteristics of basal (0 0 0 2) plane and prism (1 1 2 0) plane in HCP Zr, J. Nucl. Mater. 306 (2002) 44–53.

[63] L.G. Bland, K. Gusieva, J.R. Scully, Effect of Crystallographic Orientation on the Corrosion of Magnesium: Comparison of Film Forming and Bare Crystal Facets using Electrochemical Impedance and Raman Spectroscopy, Electrochim. Acta. 227 (2017) 136–151.

[64] K.S. Shin, M.Z. Bian, N.D. Nam, Effects of crystallographic orientation on corrosion behavior of magnesium single crys, Jom. 64 (2012) 664–670.

[65] R.C. Zeng, J. Zhang, W.J. Huang, W. Dietzel, K.U. Kainer, C. Blawert, W. Ke, Review of studies on corrosion of magnesium alloys, Trans. Nonferrous Met. Soc. China (English Ed. 16 (2006) s763–s771.

[66] X. Peng, S. Xu, D. Ding, G. Liao, G. Wu, W. Liu, Microstructural evolution , mechanical properties and corrosion behavior of as-cast Mg-5Li-3Al-2Zn alloy with different Sn and Y addition, J. Mater. Sci. & Technol. 72 (2021) 16–22.

[67] Y. Song, D. Shan, R. Chen, E. Han, Corrosion characterization of Mg – 8Li alloy in NaCl solution, Corros. Sci. 51 (2009) 1087–1094.

[68] H. Wang, Y. Song, J. Yu, D. Shan, H. Han, Characterization of Filiform Corrosion of Mg – 3Zn Mg Alloy, J. Electrochem. Soc, 164 (2017) 574–580.

[69] S. Pawar, T.J.A. Slater, T.L. Burnett, X. Zhou, G.M. Scamans, Z. Fan, G.E. Thompson, P.J. Withers, Acta Materialia Crystallographic effects on the corrosion of twin roll cast AZ31 Mg alloy sheet, Acta Mater. 133 (2017) 90–99.

[70] R.C. Zeng, Z.Z. Yin, X.B. Chen, D.K. Xu, Corrosion Types of Magnesium Alloys, Magnes. Alloy. In:T. Tanski, W. Borek, M. Krol (Eds)- Selected. Issue (2018).

[71] P. Schmutz, V. Guillaumin, R.S. Lillard, J.A. Lillard, G.S. Frankel, Influence of Dichromate Ions on Corrosion Processes on Pure Magnesium, J. Electrochem. Soc. 150 (2003) B99.

[72] C.R. McCall, M.A. Hill, R.S. Lillard, Crystallographic pitting in magnesium single crystals, Corros. Eng. Sci. Technol. 40 (2005) 337–343.

[73] M. Hoseini, P. Bocher, F. Azari, H. Vali, J.A. Szpunar, Effects of grain size and texture on the biocompatibility of commercially pure titanium, Mater. Sci. Forum. 702–703 (2012) 822–825.

[74] M. Hoseini, P. Bocher, A. Shahryari, F. Azari, J.A. Szpunar, H. Vali, On the importance of crystallographic texture in the biocompatibility of titanium based substrate, J. Biomed. Mater. Res. - Part A. 102 (2014) 3631–3638.

[75] S. Faghihi, H. vali, M. tabrizian, Effects of crystal size and orientaion of substrates on cell adhesion: implication for medical implants, Int. J. Mod. Phys. B. 22 (2012).

[76] Y. Arima, H. Iwata, Effect of wettability and surface functional groups on protein adsorption and cell adhesion using well-defined mixed self-assembled monolayers, Biomaterials. 28 (2007) 3074–3082.

[77] L.C. Xu, C.A. Siedlecki, Effects of surface wettability and contact time on protein adhesion to biomaterial surfaces, Biomaterials. 28 (2007) 3273–3283.

[78] X. Zhu, J. Chen, L. Scheideler, R. Reichl, J. Geis-Gerstorfer, Effects of topography and composition of titanium surface oxides on osteoblast responses, Biomaterials. 25 (2004) 4087–4103.

[79] Y. Kang, B. Du, Y. Li, B. Wang, L. Sheng, L. Shao, Y. Zheng, T. Xi, Journal of Materials Science & Technology Optimizing mechanical property and cytocompatibility of the biodegradable Mg-Zn-Y-Nd alloy by hot extrusion and heat treatment, J. Mater. Sci. Technol. 35 (2019) 6–18.

[80] C.L.P. Silva, A.C. Oliveira, C.G.F. Costa, R.B. Figueiredo, M.D.F Leite, M.M.Pereiral, V.F.C.Lins, T.G. Langdon, Effect of severe plastic deformation on the biocompatibility and corrosion rate of pure magnesium, J. Mater. Sci. 52 (2017) 5992–6003.

[81] S.V Dobatkin, E.A. Lukyanova, N.S Martynenko, N.Y. Anisimova, M.V. Kiselevskiy, M.V. GorshenKov, N.Y. Yurchenki. G.l. Raab, V.S. Yusupov, N. Birbilis, Strength , corrosion resistance ,

and biocompatibility of ultrafine-grained Mg alloys after different modes of severe plastic deformation, IOP Conf. Ser:Mater. Sci. Eng 194 (2017) 012004

[82]   G. B Hamu, D. Eliezer, L. Wagner, The relation between severe plastic deformation microstructure and corrosion behavior of AZ31 magnesium alloy, J. Alloys Compd. 468 (2009) 222–229.

[83]   N.N. Aung, W. Zhou, Effect of grain size and twins on corrosion behaviour of AZ31B magnesium alloy, Corros. Sci. 52 (2010) 589–594.

[84]   G. Zou, Q. Peng, Y. Wang, B. Liu, The effect of extension twinning on the electrochemical corrosion properties of Mg-Y alloys, J. Alloys Compd. 618 (2015) 44–48.

[85]   Y. Xiong, Z. Yang, T. Zhu, Y. Jiang, Effect of texture evolution on corrosion resistance of AZ80 magnesium alloy subjected to applied force in simulated body fluid, Mater. Res. Express. 7 (2020) 015406.

[86]   B.J. Wang, D.K. Xu, Y.C. Xin, L.Y. Sheng, E.H. Han, High corrosion resistance and weak corrosion anisotropy of an as-rolled Mg-3Al-1Zn (in wt .%) alloy with strong crystallographic texture, Sci. Rep. 7(2017) 16014

[87]   H. Ma, M. Liu, W. Chen, C. Wang, X. Chen, J. Dong, W. Ke, First-principles study on the effects of twin boundaries on anodic dissolution of Mg, Phys. Rev. Mater. 3 (2019) 53806.

[88]   J. Liu, E.H. Han, Y. Song, D. Shan, Effect of twins on the corrosion behavior of Mg–5Y–7Gd–1Nd–0.5Zr Mg alloy, J. Alloys Compd. 757 (2018) 356–363.

[89]   Y. Xiong, T. Zhu, J. Yang, Y. Yu, X. Gong, Effect of Twin-Induced Texture Evolution on Corrosion Resistance of Extruded ZK60 Magnesium Alloy in Simulated Body Fluid, J. Mater. Eng. Perform. 29 (2020) 5710-5717.

Figure Captions

Fig. 1. EBSD data of the as-extruded AZ31 alloy bar: (a,b) EBSD orientation maps of the LS and TS samples; (c) inverse pole figure reflecting the orientation relationship between the sample surfaces and crystal; (d,e) {0002} pole figures of the LS and TS samples [49].

Fig. 2. Different morphologies of corrosion in various crystallographic orientations. (a,c) higher index grains with terraces, (b) low index plane with filiform corrosion [62].

fig. 3. Observation of propagation of the filiform-type corrosion in the small grain sample immersed in 0.01 M NaCl + 10^{-4} M $Na_2Cr_2O_7$ solution. (a) *in situ* optical observation (arrows indicate propagation direction), (b) SEM observation directly after solution emersion [70].

Fig. 4. Optical micrographs showing the microstructures of AZ31B-H24 alloy at different heat treated conditions: (a) HT 200, (b) HT 300 [82].

Fig. 5. The EBSD results for the Mg-4Zn alloy after immersion in PBS. Twins are marked by arrows [10].

Fig. 6. Optical microscopy micrographs of the EW75 alloy after: (a) T4 treatment (solid solution treated), and (b) T3 treatment (compressed at room temperature) [87].

Fig. 7. *In situ* optical observation of the filiform-type corrosion on a twin of the large grain sample immersed in 0.01 M NaCl + 10^{-4} M Na_2Cr_2O7: (a) initiation and initial propagation, and (b) behavior upon intersection of two twins [70].

Fig. 8. Optical micrograph of corrosion in a twinned grain of Mg. Note that the thick twin continues, unattacked, through the region of corrosion near the center of the micrograph. Schematic unit cells of the grain and twin are from OIM analyses [70].

Table Captions

Table. 1. Summary of texture effect on the corrosion films of Mg and its alloys in different corrosive media

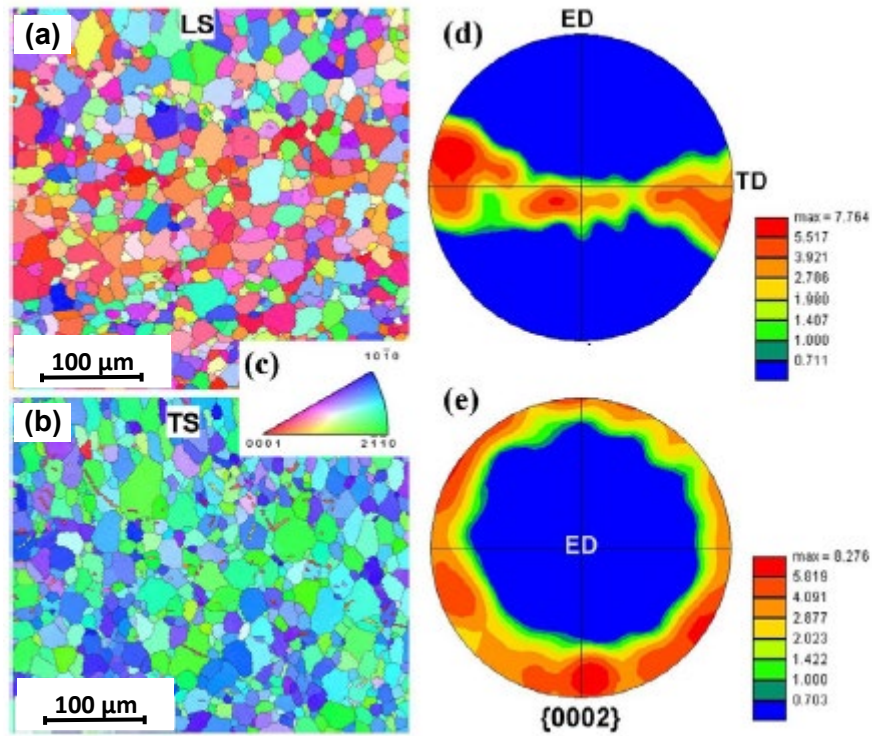Table 2. Summary of the effect of twinning on the corrosion resistance of the Mg alloys

Fig. 1. EBSD data of the as-extruded AZ31 alloy bar: (a,b) EBSD orientation maps of the LS and TS samples; (c) inverse pole figure reflecting the orientation relationship between the sample surfaces and crystal; (d,e) {0002} pole figures of the LS and TS samples [49].
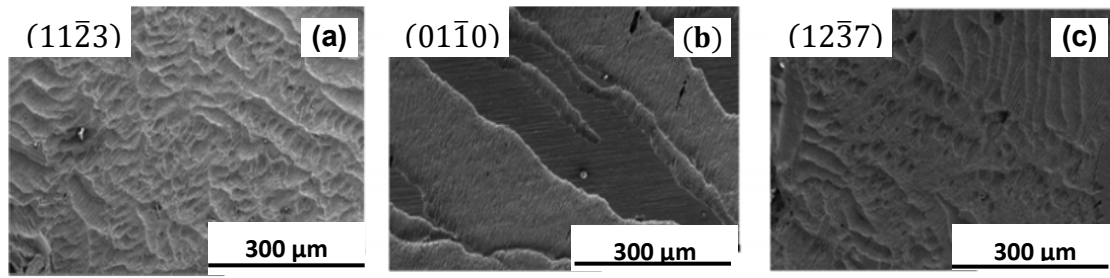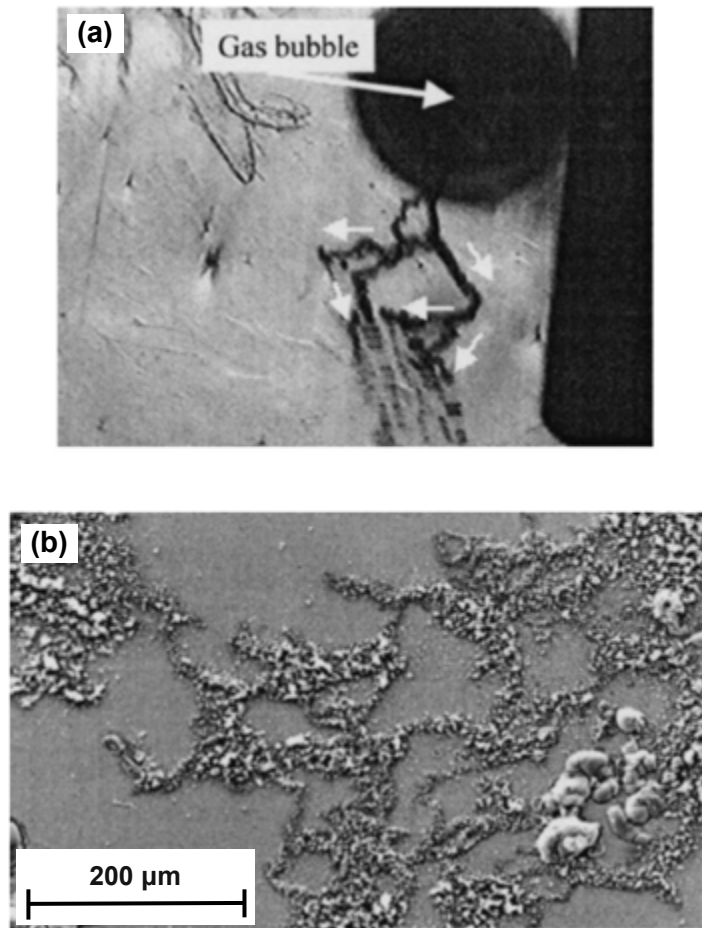
Fig. 2. Different morphologies of corrosion in various crystallographic orientations. (a,c) higher index grains with terraces, (b) low index plane with filiform corrosion [62].

Fig. 3. Observation of propagation of the filiform-type corrosion in the small grain sample immersed in 0.01 M NaCl + 10^{-4} M $Na_2Cr_2O_7$ solution. (a) *in situ* optical observation (arrows indicate propagation direction), (b) SEM observation directly after solution emersion [70].
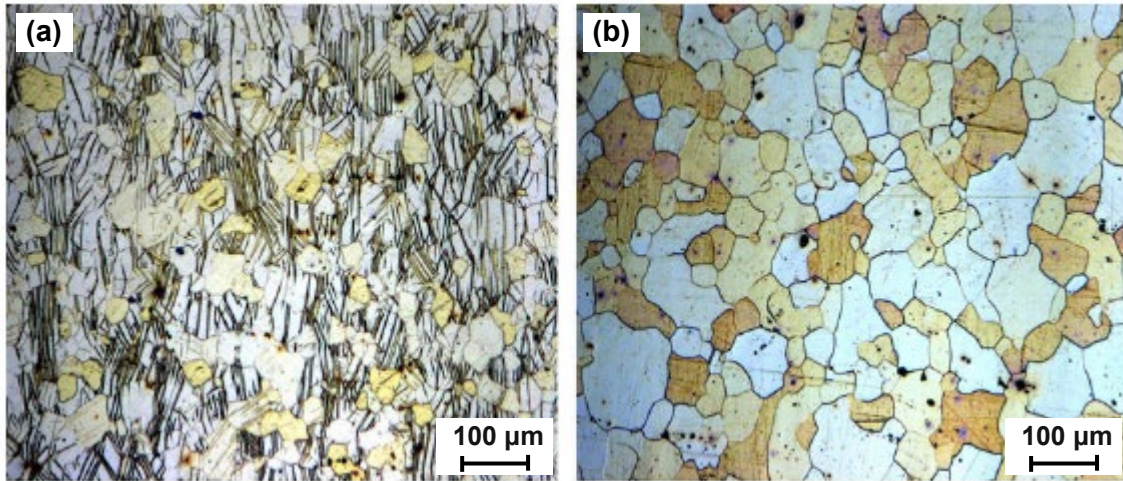
Fig. 4. Optical micrographs showing the microstructures of AZ31B-H24 alloy at different heat treated conditions: (a) HT 200, (b) HT 300 [82].
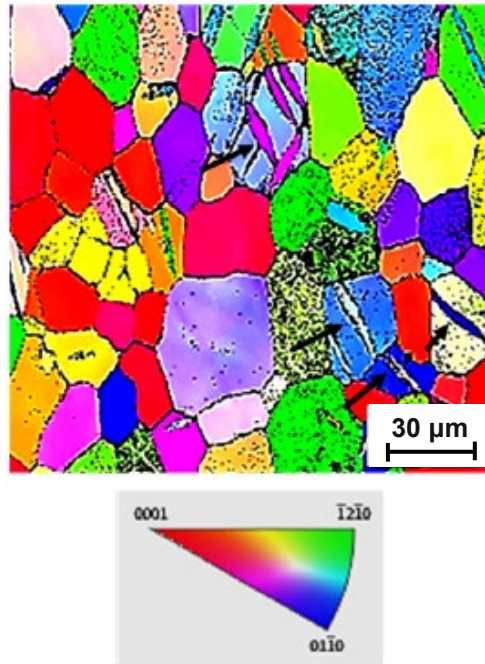
Fig. 5. The EBSD results for the Mg-4Zn alloy after immersion in PBS. Twins are marked by arrows [10].
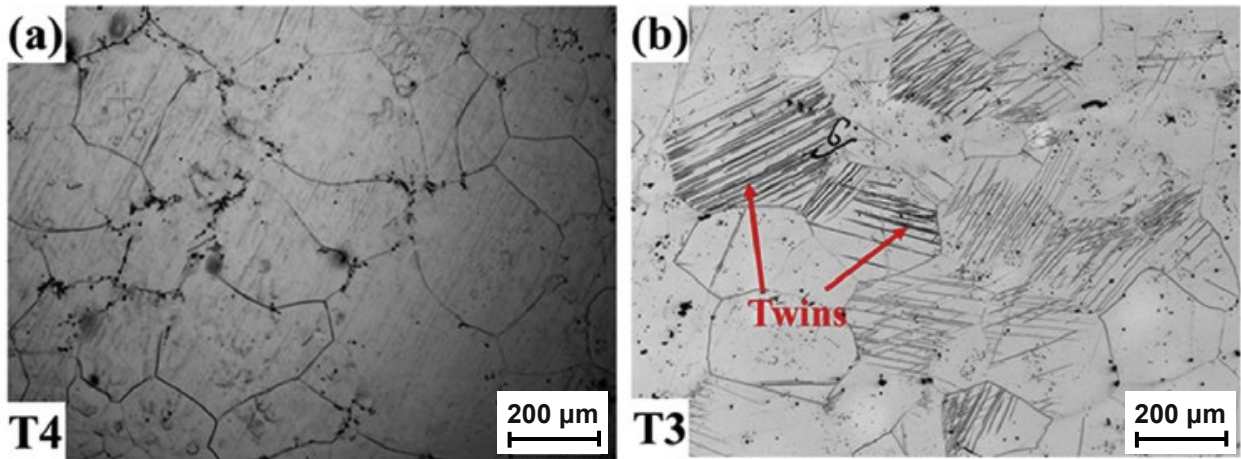
Fig. 6. Optical microscopy micrographs of the EW75 alloy after: (a) T4 treatment (solid solution treated), and (b) T3 treatment (compressed at room temperature) [87].
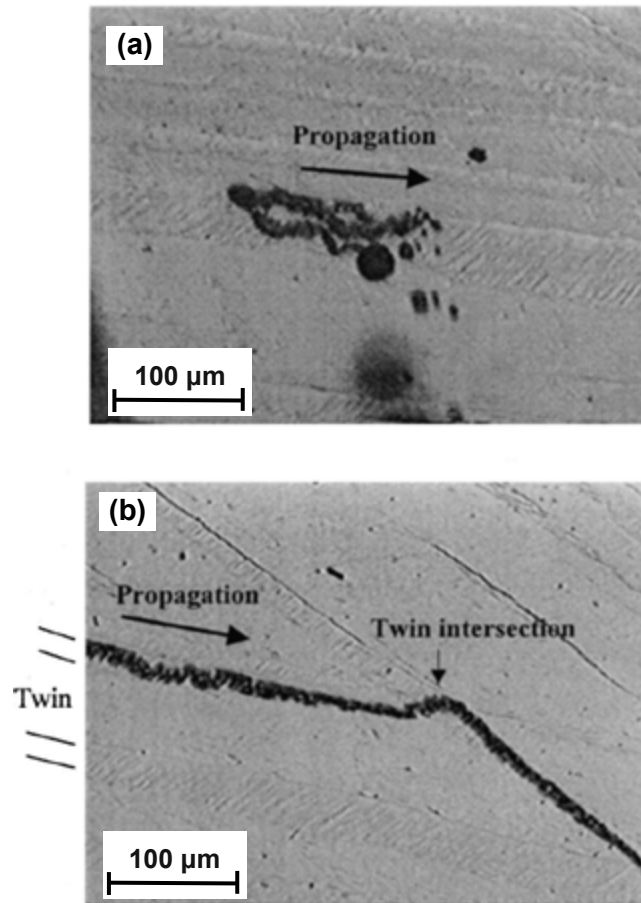
Fig. 7. *In situ* optical observation of the filiform-type corrosion on a twin of the large grain sample immersed in 0.01 M NaCl + 10^{-4} M Na_2Cr_2O7: (a) initiation and initial propagation, and (b) behavior upon intersection of two twins [70].
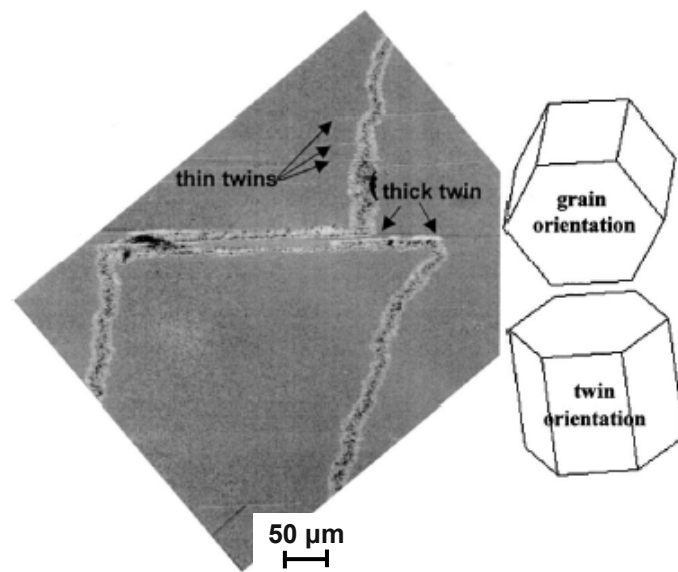
Fig. 8. Optical micrograph of corrosion in a twinned grain of Mg. Note that the thick twin continues, unattacked, through the region of corrosion near the center of the micrograph. Schematic unit cells of the grain and twin are from OIM analyses [70].

Table. 1. Summary of texture effect on the corrosion films of Mg and its alloys in different corrosive media

Material	Corrosion media	Corrosion test	Effect of texture on corrosion films	Reference
Pure Mg	Hank solution	EIS[1], polarization, H_2 evolution	Film formed on basal plane is more protective.	[44]
AZ31	PBS	Polarization, H_2 evolution	For $\{10\bar{1}0\}$ and $\{11\bar{2}0\}$ prism planes, the film could keep good protection. But for $\{0002\}$ basal planes, $\{10\bar{1}0\}$ and $\{11\bar{2}0\}$ prism planes, the film degraded widely.	[50]
Pure Mg	$Mg(OH)_2$ and NaCl	EIS, SKP[2], SVP[3]	Film formed on basal planes is more compact and protective.	[59]
Pure Mg	TRIS, EDTA	EIS, RVS[4]	Film formed on prismatic planes is thicker and more resistant.	[62]
Pure Mg	3.5% NaCl	polarization, EIS	Film formed on low-index plane is a more effective barrier against penetration of color ions.	[63]

[1] EIS: Electrochemical impedance spectroscopy
[2] SKP: Scanning Kelvin Probe
[3] SVP: Scanning Vibrating Probe
[4] RVS: Raman Vibrational Spectroscopy

Table 2. Summary of the effect of twinning on the corrosion resistance of the Mg alloys

Material	Processing route	Environment	Corrosion test	Effect of twinning on corrosion resistance	Reference
Mg-4Zn	Extrusion	PBS	Polarization	Optimum amount is required	[10]
Mg-3%Al-1%Zn	Extrusion	0.9% NaCl	Polarization, EIS, H_2 evolution	Complicated results	[49]
AZ31	Rolling	5% NaCl	EIS, H_2 evolution	Does not have a decisive influence	[40]
AZ31	ECAE	3.5% NaCl	Polarization	decreased	[81]
AZ31B	Rolling	3.5% NaCl	Polarization, H_2 evolution	decreased	[82]
Mg-Y	Compression	0.9% NaCl	Potentiostat/FRA*	increased	[83]
AZ80	Rolling and compression	SBF	EIS	increased	[84]
EW75	Compression	3.5% NaCl	Weight loss, EIS	increased	[87]
ZK60	Extrusion	SBF	Polarization, EIS	Decreased with small amount, and increased with high amount of twins.	[88]

*frequency response analysis